Distribution Agreement

In presenting this thesis as a partial fulfillment of the requirements for a degree from Emory University, I hereby grant to Emory University and its agents the non-exclusive license to archive, make accessible, and display my thesis in whole or in part in all forms of media, now or hereafter now, including display on the World Wide Web. I understand that I may select some access restrictions as part of the online submission of this thesis. I retain all ownership rights to the copyright of the thesis. I also retain the right to use in future works (such as articles or books) all or part of this thesis.

Jerry William Allen April 8, 2019

Investigating the Interaction of Upregulated Signaling Effectors in GBM

by

Jerry William Allen

Dr. Renee Read
Adviser

Pharmacology and Chemical Biology

Dr. Renee Read

Adviser

Dr. Steven Sloan

Committee Member

Dr. Eladio Abreu

Committee Member

Dr. Matthew Weinschenk

Committee Member

2019

Investigating the Interaction of Upregulated Signaling Effectors in GBM

By

Jerry William Allen

Dr. Renee Read

Adviser

An abstract of
a thesis submitted to the Faculty of Emory College of Arts and Sciences
of Emory University in partial fulfillment
of the requirements of the degree of
Bachelor of Sciences with Honors

Department of Biology

2019

Abstract

Investigating the Interaction of Upregulated Signaling Effectors in GBM
By Jerry William Allen

Glioblastoma Multiforme (GBM) is the most common primary malignant brain tumor in adults worldwide and arises in glial cells and glial progenitors with a median over-all survival of those diagnosed being 15 months despite treatment. Despite extensive research on common genetic lesions that occur in GBM, such as overactivity of the RTK and PI3K signaling pathways, current therapies designed to target these known mechanisms are ineffective at treating the disease. Using a novel *Drosophila* GBM model, previous work in our laboratory identified Right Open Reading Frame 2 (dRIOK2) as an essential component of tumor cell maintenance and survival in RTK-PI3K-driven GBM. dRIOK2 is a highly conserved atypical serine-threonine kinase involved in ribosomal maturation with a known human ortholog, RIOK2. To understand downstream targets of RIOK2, we analyzed proteomic data from immunoprecipitation experiments of kinase-active and kinase-dead RIOK2 in a cultured-human GBM cell line and uncovered that kinase-active RIOK2 interacts with the RNA-binding protein IMP3, whose functions include the trafficking and translation of oncogenic mRNA such as *MYC*, *IGF2*, and *CyclinD1*. These data suggest a potential mechanism of the RIOK2-dependence observed in the *Drosophila* GBM model and validated in cultured human GBM cells. To investigate this potential relationship between RIOK2 and IMP3, we initially screened publicly-available expression data from the Cancer Genome Atlas (TCGA) and other databases by glioma grade and *IDH1*-mutant status. Preliminary data suggested RIOK2 and IMP3 were overexpressed in GBM, which we sought to validate using immunohistochemistry on tumor tissue microarrays to probe for co-overexpression of each protein in the same tissue samples. As a next step in our investigations of RIOK2 and IMP3, we will look to recapitulate the RIOK2-dependence findings from the *Drosophila* and human-cultured-cells GBM models in an inducible murine GBM model.

Investigating the Interaction of Upregulated Signaling Effectors in GBM

By

Jerry William Allen

Dr. Renee Read

Adviser

A thesis submitted to the Faculty of Emory College of Arts and Sciences
of Emory University in partial fulfillment
of the requirements of the degree of
Bachelor of Sciences with Honors

Department of Biology

2019

Acknowledgements

First and foremost, I would like to thank my research advisor Dr. Renee Read for providing me with the opportunity to be a part of such a wonderful and dynamic lab environment over the past six months. I remember how nervous I was when I first joined the lab, but everyone was extremely supportive from the first day and I could not have wished for a better set of role models. I would also like to extend a special thanks to my research mentor Dr. Nathaniel Boyd, whose patience and support were amongst the greatest driving forces to the development of my confidence in the lab. Each person in the lab provided support at some stage that was vital to my progress throughout the project, for which I thank Dr. Se-Yeong Oh, Alexander Chen, Leon McSwain, Marin Miller, and Riley Gulbronson.

Additionally, I extend my sincere gratitude to each of my committee members, Dr. Steven Sloan, Dr. Eladio Abreu, and Dr. Matthew Weinschenk, for the commitment of their time and support for my project, as well as their mentorship throughout my undergraduate experience.

I am also grateful for the love and support of my family members and close friends, without whom I would not have had the foundational encouragement that bolstered the completion of this work.

The results shown here are in part based upon data generated by the TCGA Research Network: https://www.cancer.gov/tcga.

TABLE OF CONTENTS

INTRODUCTION

Glioblastoma Multiforme Epidemiology & Etiology

The nervous system is composed of neuronal cells and glial cells. Glial cells perform a variety of essential functions in the nervous system and are categorized into four groups: microglia, astrocytes, oligodendrocytes, and their progenitor cells (Jakel and Dimou, 2017). The term glioma broadly refers to primary brain cancers that arise in one or more of these cellular subcategories (Hanif et al., 2017).

The World Health Organization (WHO) categorizes gliomas according to four grades: I, II, III, and IV, with grades I and II composing the classification of low-grade gliomas while grades III and IV constitute high-grade gliomas, or malignant gliomas (Louis et al., 2007). Although relatively rare, malignant gliomas represent the majority of all primary brain tumors and correspond to a profound morbidity rate (Jovcevska et al., 2013; Wen and Kesari, 2008).

Glioblastoma Multiforme (GBM), a highly-proliferative malignant neoplasm derived from glial cells and their precursors, is the only astrocytoma classified as grade IV (Louis et al., 2001). It is the most common and most aggressive form of primary brain cancer in adults and remains incurable by current therapies. Fewer than 10 people per 100,000 develop GBM globally, generally at an age around late 50's and early 60's (Ohgaki and Kleihues, 2005). There are not many well-established risk factors for developing GBM other than high-dose radiation and hereditary predisposition, although there is a higher incidence rate among males conferring some gender-associated risk (Bondy et al., 2008). Additionally, there is data to suggest that females who do develop GBM tend to have comparatively better survival rates to males (Tian et al., 2018). Currently, the standard of care therapy for GBM consists of maximal surgical resection followed by concomitant radiation treatment and chemotherapy with the alkylating

agent temozolomide, yet the disease prognosis remains poor with median over-all patient survival being 15 months after diagnosis despite treatment (Hanif et al., 2017).

The latest edition of the WHO Classification of Tumors of the Central Nervous System (CNS), published in 2016, continues to emphasize histological characteristics as the basis of identifying GBM, though with an added subcategorization determined by mutation-status in *IDH1/2* and other loci, which signal important differences in patient outcome (Komori, 2017). Normally, *IDH1/2* proteins catalyze the production of α-ketoglutarate (αKG) from isocitrate and generate NADPH; however, when mutated, isocitrate dehydrogenase (IDH) 1 and 2 proteins catalyze the production of an oncometabolite, 2-hydroxyglutarate, from αKG, and lack NADPH production (Cohen et al., 2013). *IDH1/2*-mutant status generally corresponds with a better prognosis than *IDH1/2*-wild-type status and occurs at a greater relative frequency in secondary GBM, in which a lower-grade glioma develops into grade IV (Ohgaki and Kleihues, 2013).

Although classification of GBM remains predominantly histological, there are also other common genetic lesions like *IDH1/2*-mutant status that are well documented. Amplifications, overexpression, and/or mutations in receptor tyrosine-kinases (RTKs), such as EGFR or PDGFRA, and other mutations that result in aberrant PI-3 kinase (PI3K) signaling are frequently found in GBM, such as loss-of-function mutations in the *PTEN* PI-3 lipid phosphatase and tumor suppressor but are far less frequently found in lower grade gliomas (Brennan et al., 2013; Cancer Genome Atlas Research, 2008). However, despite this knowledge, effective targets for treating GBM have not been found.

Targeted therapies directed at RTKs and PI3K pathway effectors, such as mTOR, have not been effective, which suggests yet-to-be-discovered underlying mutations and mechanisms responsible for the maintenance of GBM malignancy (Cloughesy et al., 2008; MacDonald et al.,

2011). Furthermore, considering the overlap of aberrant mutations and signaling pathways occurring between GBM and other distinct cancers, such as non-small-cell lung cancer, HER2-positive breast cancer, and colorectal cancers, a greater understanding of how the modules associated with RTK and PI3K pathways are regulated may provide an invaluable foundation for the development of better-informed future investigations across malignancies (Regad, 2015).

Background & Preliminary Data

To screen for potentially disease-specific signaling effectors associated with RTK and PI3K pathways, our laboratory established a *Drosophila melanogaster* fly model wherein overactive EGFR and PI3K signaling in glial progenitor cells generates GBM-like neoplastic glia (Read et al., 2009). We then screened for potential pathway effectors that were necessary for the maintenance of the neoplastic state. This project focused on kinases because of their druggable nature, the fact that *Drosophila* have clear human orthologs for all of their kinases, and that kinase structure is well-understood. Using RNA interference (RNAi) to target most kinases in the *Drosophila* genome in the GBM-fly model, we identified the atypical serine-threonine kinase *dRIOK2,* or *Drosophila* right-open reading frame kinase 2, as a target for further investigation because *dRIOK2* knockdown caused tumor-cell specific synthetic lethality in the context of EGFR signaling (Read et al., 2013).

Further investigation led to the discovery that the catalytic activity of RIOK2 protein, which is the human ortholog of dRIOK2, was necessary for GBM tumor cell growth and survival. In contrast, the catalytic activity of other RIO family kinases, such as RIOK1, was not required for tumor cell growth. Though the function of RIOK2 in the RTK and PI3K pathways is not understood, preliminary proteomic analysis of RIOK2-binding proteins in GBM tumor cells

performed in our laboratory revealed interactions between RIOK2 and multiple RNA-binding proteins (RBPs). Amongst these RBPs was the protein IGF2BP3, also known as IMP3, which selectively binds to kinase-active RIOK2, but not to kinase-dead (Table 1). IMP3 selectivity in associating with RIOK2 suggests a relationship between this RBP and RIOK2 activity regulated downstream of RTK-PI3K signaling in GBM tumor cells. Consistent with this hypothesis, RNAi of Imp, which encodes the *Drosophila* ortholog of IMP3, also caused tumor-cell-specific synthetic lethality in the context of EGFR signaling in our *Drosophila* model of GBM.

	RIOK2	RIOK2-flag	RIOK2KD-flag	IGG control
RIOK2	22	78	78	0
RNA-binding proteins				
IMP3	8	5	0	0
G3BP2	8	6	6	0
ATXN2L	8	8	10	2
ILF3	17	4	11	0
RIOK2-binding Ribosome Assembly factors				
TSR1	30	18	6	0
LTV1	21	8	11	0
NOB1	12	7	8	0
PNO1	18	11	12	0
BYSL	17	4	2	0

Table 1: Proteomic profiling of RIOK2 IPs in GBM. Numbers for each protein show total spectral counts from RIOK2 and associated proteins in IPs. RIOK2 significantly associates with RNA-binding proteins and ribosome assembly factors.

As a member of the IMP family of RNA-binding proteins, IMP3 plays an important role in the trafficking and translational initiation of select target mRNAs during development, especially in the nervous system (Bell et al., 2013). IMP3 mRNA targets include *IGF2*, *CD44*, *MYC*, and *CyclinD1*, whose associated protein functions include promotion of proliferation and growth in developing tissues and, in tumor cells, promotion of cancer progression and therapeutic resistance, which reflect the role of IMP3 as a driver of tumorigenesis in GBM and

other tumor types (Lederer et al., 2014; Palanichamy et al., 2016). Furthermore, constitutive RTK-PI3K signaling is associated with transcriptional overexpression of many known IMP3 target mRNAs that encode established drives of gliomagenesis (Suvasini et al., 2011). Further exploration of the mechanistic interactions between RIOK2 and IMP3 could provide a better understanding of the exact role that RIOK2 plays in RTK and PI3K signaling and, thus, a better understanding of the pathway as it functions in GBM.

Hypothesis & Approach

Based on our preliminary data connecting active RIOK2 with IMP3 function in GBM cells and based on published literature on the oncogenic mRNA targets of IMP3, I hypothesize that oncogenic RTK-PI3K signaling activates RIOK2 to drive GBM via binding to and activating IMP3 to promote translation of oncogenic target mRNAs that themselves are expressed downstream of oncogenic RTK-PI3K signaling in tumor cells. In this way, RIOK2 acts at a key tumor-cell-specific regulatory step in RTK-PI3K-mediated transformation of glial cells.

If RIOK2 and IMP3 function within the same pathway in RTK-PI3K driven GBM tumors, then we would expect these proteins to be co-expressed within GBM cells along with their associated downstream effector proteins such as MYC, Cyclin D1, and CD44. Thus, we probed for the co-expression of RIOK2 and IMP3 through immunohistochemistry (IHC) to determine if there was a correlation between expression levels of each protein. IHC was conducted on consented GBM tumor specimens with corresponding clinical history and diagnostic information provided through our lab's participation in the IRB-approved (protocol IRB00045732) Emory University Brain Tumor Sample and Information Resource (BTSIR). Results for IMP3 and RIOK2 staining from IHC were scored by myself and validated by Dr.

Nathaniel Boyd and neuropathologist Dr. Stewart Neill. The scoring results from the IHC data were analyzed for a correlation between RIOK2 and IMP3 expression amongst the same tumor samples and juxtaposed to their known genomic alterations.

In addition, existing genomic and phenotypic data from the Cancer Genome Atlas (TCGA) database and additional data on gliomas from the Gravendeel dataset were screened and downloaded through the GlioVis data-portal and analyzed via GraphPad software (Bowman et al., 2017; Cancer Genome Atlas Research et al., 2013; Gravendeel et al., 2009). Specifically, mRNA expression for a variety of associated RTK-PI3K signaling modules was measured between categorizations that included *IDH1/2*-mutant status and glioma grade to generate a baseline understanding of potential correlations from the existing data. According to preliminary analyses, there are correlations between higher mRNA expression levels *RIOK2*, *IMP3*, and genes that encode IMP3 target mRNAs in GBMs.

While patient-derived xenograft models of GBM represent an important model to recapitulate the tumor microenvironment better than cell culture systems, drawbacks include the inability to study tumor initiation as well as interactions with the immune system in the tumor microenvironment.

Considering these limitations, an additional aspect of our investigations on RIOK2 includes validating preliminary findings that RIOK2 is important for tumor maintenance in murine GBM models with the goal of examining RIOK2 dependence in tumors that arise from glial cells within the brain parenchyma in the context of a functional immune system. The mouse model for these experiments is an RCAS-/tv-a mouse model system of GBM co-developed by our collaborator Dr. Dolores Hambardzumyan that incorporates the reliable and reproducible RCAS-/tv-a retrovirus system which is used to engineer GBM-like tumors from endogenous

neuro-glial progenitor cells in the mouse brain (Becher et al., 2008; Hambardzumyan et al., 2009; Pitter et al., 2016; Szulzewsky et al., 2015).

As an extended part of my project and with the aid of my postdoc research mentor Dr. Nathaniel Boyd, we aim to screen and validate lentiviral shRNA constructs to knockdown RIOK2 in mouse neuro-glial progenitor cells *in* vitro to identify the most effective shRNA sequence for use *in vivo* with the RCAS/tv-a system. We measured the effect of different shRNAs on relative expression of RIOK2 via qPCR of two separate mouse neural stem cell (mNSC) lines infected with different lentiviral constructs and analyzed the knockdown relative to a control construct encoding green fluorescent protein (GFP).

Our murine GBM models involve transducing neuro-glial progenitor cells with tumorigenic EGFR mutations with either a lentiviral or RCAS shRNA construct that will knockdown expression of RIOK2 in GBM tumor cells in order to test whether RTK-driven murine GBM cells are dependent on RIOK2 function for their proliferation and survival, and to determine if RIOK2 dependence is evolutionarily recapitulated in mouse GBM models as we observed between *Drosophila* neoplastic glia and human cultured GBM stem cell models. Furthermore, determining that RIOK2 is necessary for maintenance of a tumorigenic phenotype in murine GBM would open the validity of this model to further exploration of the mechanistic interaction between RIOK2 and IMP3 function *in vivo*.

METHODS & MATERIALS

The Cancer Genome Atlas (TCGA) & Assorted Database Analysis of Co-Expression

All expression data for gliomagenic genes of interest was gathered from the online data portal GlioVis, which includes entire datasets from a wide-array of databases (Bowman et al., 2017). To compare the mRNA expression levels of loci that encode different RTKs like EGFR and PDGFRA and signaling effectors RIOK2 and IGF2BP3 (IMP3) across glioma grades, the raw RNA-Seq TCGA dataset 'TCGA_GBMLGG' was downloaded. This set includes expression data for low-grade gliomas (LGG) and GBM across various target genes and was plotted as box-and-whisker graphs with GraphPad. Statistical analysis was conducted by GraphPad software using Welch's t-tests between glioma grades at a 95% confidence interval, considering that the number of samples per grade varied. Generally, data for only grades III and IV were subject to statistical analysis in order to determine the degree of difference between GBM and other high-grade gliomas (HGGs).

Expression data separated by *IDH1*-mutant status was obtained through GlioVis from the Gravendeel dataset, which also includes *IDH1*-mutant status across glioma grade (Gravendeel et al., 2009). Data was processed to only incorporate grade IV samples and was plotted as a box-and-whisker graph between *IDH1*-mutant and *IDH1*-wild-type. Welch's t-tests were used to analyze the statistical significance of any difference in expression between the two groups across the selected genes.

Immunohistochemistry and processing of Tumor microarray

All the tumor samples used for the tumor microarray (TMA) procedure were donated surgical specimens of human tumor with written informed consent of patients in the IRB-approved protocol (IRB00045732) approved by Emory University's Institutional Review Board, as previously described (Chen et al., 2019). Paraffin-embedded TMA slides were provided through the Winship Core Pathology Laboratory and included matched normal brain control tissue.

IHC and antigen retrieval for the RIOK2 antibody (1:125, Sigma Prestige, HPA005681) were completed according to the general protocol for the ImmPRESS® HRP Anti-Rabbit Detection Kit by Vector Laboratories (cat. No. MP-7401), with minor time adjustments at between washes and rehydration steps to optimize development. Similar time adjustments were made for the IMP3 antibody (1:250, Dako, M3626) using the ImmPRESS® HRP Anti-Mouse Detection Kit (cat. No. MP-7402) also by Vector Laboratories.

TMA slides were scored according to standard clinical criteria according to a scale of 0 (no stain), 1 (light staining), 2 (intermediate staining), and 3 (strong staining) and images of representative IHC samples were taken on an Olympus DP72 CCD camera at a 20x magnification and an exposure time of 15.31 ms. Additionally, all images were taken at the same time to control for lighting conditions as much as possible. Selected images were taken of samples derived from the same sources between slides to compare expression staining of similar tissue. Once all available samples had been scored, the proportion of control tissue per score was plotted alongside the proportion of tumor tissue per score for each antibody target and graphed via GraphPad. Pseudonyms were assigned to each sample designating whether it was normal

brain control tissue (N) or tumor tissue (T) and a number to distinguish between different samples of the same categorization.

qPCR for Validating *in vitro* Viral shRNA Knockdown

Third-generation lentiviral production is done by transfecting a human embryonic kidney cell line of 293T cells, we used CSC 293 cells developed by Hjelmeland laboratory, with three separate plasmids each containing functional components of the lentiviral system (Walker and Hjelmeland, 2014). CSC 293 cells are initially grown in a stem cell media without antibiotic and then transfected with a non-supplemented stem cell media mixture including a plasmid containing the gene for a packaging protein, pCMV-dR8.2 dvpr [1], a plasmid containing the gene for an envelope protein, pCMV-VSV-G[2], a plasmid containing a gene for the shRNA of interest, and ViaFect™ Transfection Reagent (Promega, E498A). One day after the transfection process, the media is swapped for supplemented stem cell media. A day or two later, media is collected via a filtered .45-micron syringe and should contain the desired viral product produced by the transfected cells.

To validate RIOK2 shRNAs, we tested *Ink4a/arf*$^{-/-}$ mouse neural stem cells (mNSCs), which are non-tumorigenic immortalized neural stem cells cultured from neonatal P0-P1 mouse pups, and *Ink4a/arf*$^{-/-}$; *PTEN*$^{-/-}$; *EGFR*^{vIII} murine GBM stem cells (mGSCs), which are tumorigenic murine neonatal neural stem cells that express the oncogenic EGFRvIII mutant variant found in human GBM. mNSCs and mGSCs were were grown in a DMEM/F12 stem cell

[1] pCMV-dR8.2 dvpr was a gift from Bob Weinberg (Addgene plasmid # 8455 ; http://n2t.net/addgene:8455 ; RRID:Addgene_8455)

[2] pCMV-VSV-G was a gift from Bob Weinberg (Addgene plasmid # 8454 ; http://n2t.net/addgene:8454 ; RRID:Addgene_8454)

media with pyruvate and glutamax (Gibco/Life Technologies 10565) supplemented with B27 (Cat #17504-044), bFGF, EGF, heparin, and 100x pen/strep antibiotic. Cells were passaged generally every 5 days as a 1:10 dilution. Before infection with lentivirus, the cells were grown out until there were enough cells to plate approximately two million onto three separate plates. Each plate was than infected with a separate lentivirus, one containing GFP as control, and the other two containing different forms of RIOK2 short hairpin RNA (shRNA). To maximize infection efficiency, the plates were infected over multiple days and then harvested for their mRNA.

Reverse-transcriptase quantitative PCR (RT-qPCR) was then performed on the extracted mRNA from each cell type infected by the different lentiviral constructs using primers for mRIOK2 (IDT, forward '5- GGCTTTACTTATCTCGGCTCTC -3', reverse '5- TGATCACTGCATGGCGATTA -3') and mActinB (IDT, forward '5- GGCTGTATTCCCCTCCATCG -3', reverse '5- CCAGTTGGTAACAATGCCATGT -3'). Raw data was then calculated using the delta-delta Ct method which can be used to compare the relative expression of different genes between samples. The resultant data was statistically analyzed using Welch's t-test between groups and graphed through GraphPad.

RESULTS

Database Analysis

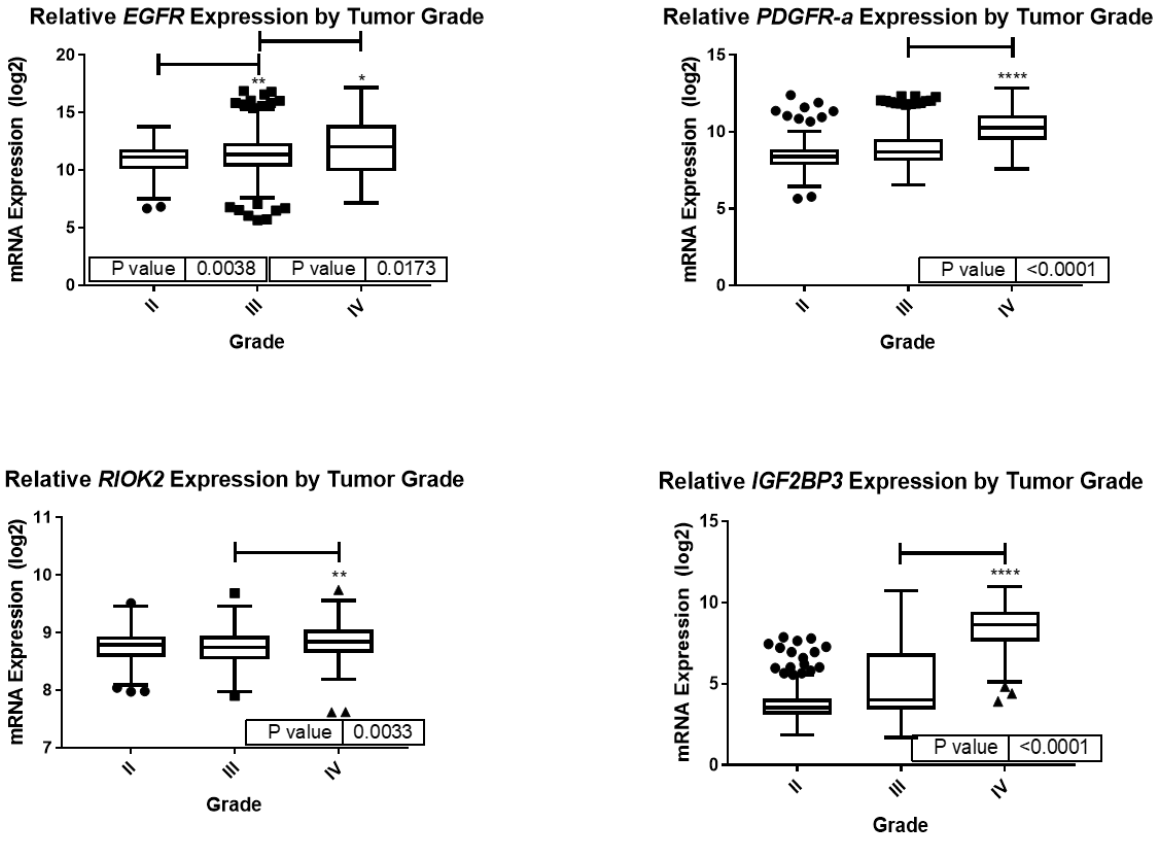

Figure 1. mRNA expression data from RNA-Seq for EGFR (top-left), PDGFR-a (top-right), RIOK2 (bottom-left), and IGF2BP3 (IMP3, bottom-right) in patient samples from the Cancer Genome Atlas (TCGA) by glioma grade.

Our initial screening of TCGA data looked at the expression data for *EGFR* (top-left), *PDGFR*-α (top-right), *RIOK2* (bottom-left), and *IMP3* (bottom-right) across glioma grades II, III, and IV (Figure 1). Specifically, all expression data plotted for Figure 1 was obtained from the 'TCGA_GBMLGG' dataset on GlioVis. Statistical analysis between grades was only conducted between grade III and IV for all mRNA of interest, except for *EGFR*, using Welch's t-tests and the overhead bars with asterisk symbols represent a difference between the sample populations that is statistically significant. Of the statistical analysis conducted, the general trend is an expected

increase in expression as grade of the glioma increases. Between grades III and IV, there is a statistically significant difference in expression of *EGFR* (p=0.0173), *PDGFR-a* (p<0.0001), *RIOK2* (p=0.0033), and *IMP3* (p<0.0001). The most significant increase in expression from grade III to grade IV is noticed in *IMP3* mRNA expression levels.

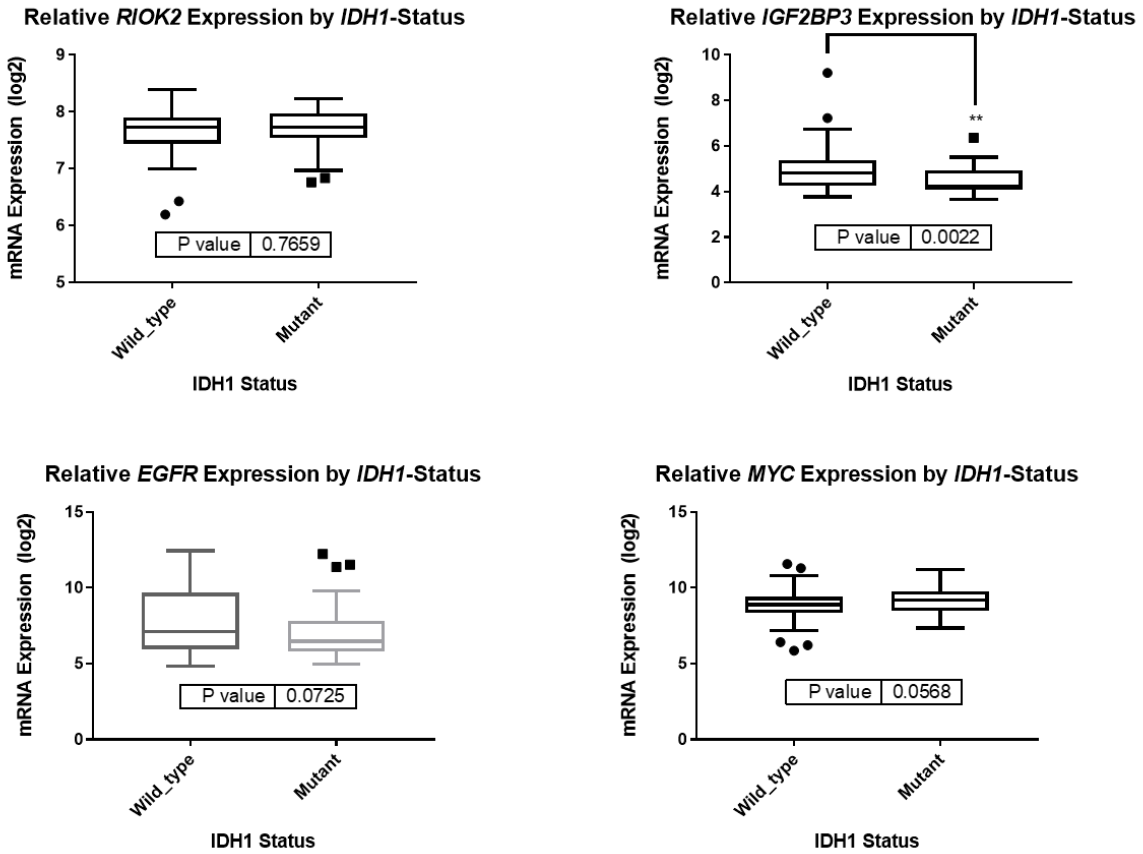

Figure 2. mRNA expression data for RIOK2 (top-left), IGF2BP3 (IMP3, top-right), EGFR (bottom-left), and MYC (bottom-right) in Grade IV patient samples from the Gravendeel dataset by *IDH1*-mutant status.

After looking at expression by glioma grade, we were interested in comparing the expression levels of *RIOK2*, *IMP3*, *EGFR*, and *MYC* between *IDH1*-wild-type GBM and *IDH1*-mutant GBM to look for any significant trends within the available data (Figure 2). Expression data by *IDH1*-mutant status was graphed from the Gravendeel dataset obtained through the GlioVis portal and processed to only include information from grade IV gliomas for a total of 95

wild-type samples and 33 mutant samples (Gravendeel et al., 2009). Welch's t-test was used to identify statistically significant differences in expression of *RIOK2* (p=0.7659), *IMP3* (p=0.0022), *EGFR* (p=0.0725), and *MYC* (p=0.0568) between *IDH1*-mutant and *IDH1*-wild-type tumors. The only statistically significant difference observed was found for the expression levels of *IMP3*, which showed a decrease in *IMP3* mRNA expression in *IDH1*-mutant tumors relative to *IDH1*-wild-type tumors.

qPCR of shRNA Infected mNSCs

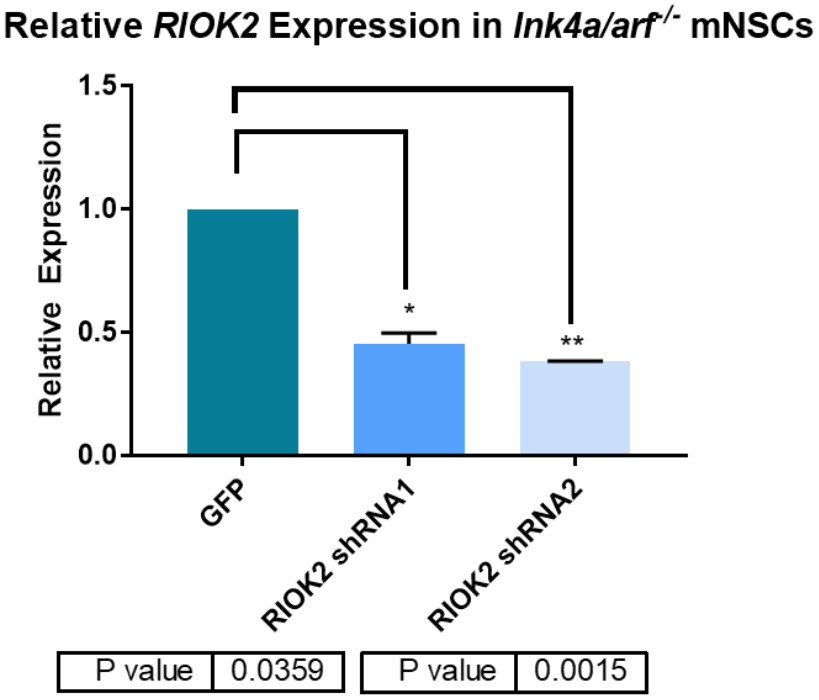

Figure 3. Relative expression of *RIOK2* in *Ink4a/arf*$^{-/-}$ mNSCs infected with lentivirus containing GFP or two different types of RIOK2 shRNA are plotted in a bar graph to illustrate the differences between each group. Bars connecting groups represent statistically significant differences relative to the control while the number of asterisks indicates the degree of significance. P-values for conducted t-tests are also included for each bar.

Following the database screening and analysis of available expression data, we wanted to determine which of the available RIOK2 shRNA that we had in lab was most effective at knocking down *RIOK2* expression *in vitro*. Beginning with *Ink4a/arf*$^{-/-}$ mNSCs, Welch's t-tests between cells infected with one of two RIOK2 shRNA and those infected with the GFP control were performed to determine if the shRNA had a significant effect in knocking down *RIOK2* mRNA expression (Figure 3). Both the RIOK2-shRNA1 (p=0.0359) and the RIOK2-shRNA2 (p=0.0015) groups showed a statistically significant reduction in relative expression of *RIOK2*, with the cells infected with RIOK2-shRNA2 seeing a greater reduction than those of RIOK2-shRNA1.

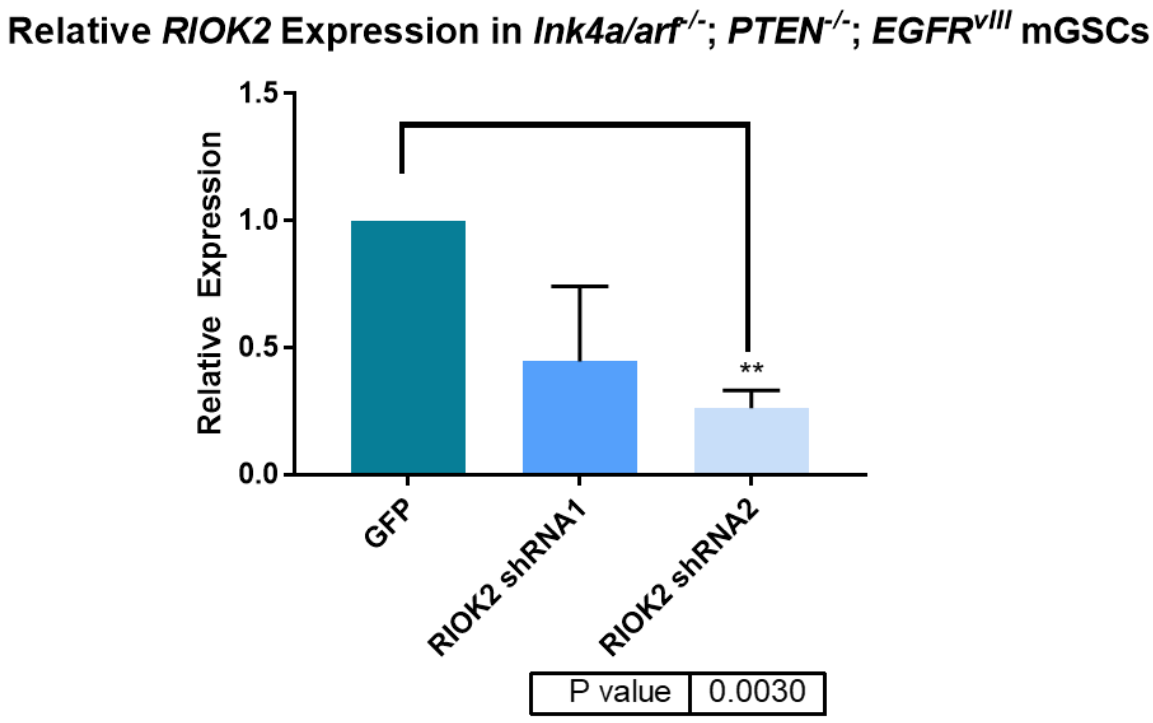

Figure 4. Relative expression of *RIOK2* in *Ink4a/arf*$^{-/-}$; *PTEN*$^{-/-}$; *EGFR*^{vIII} mGSCs infected with lentivirus containing GFP or two different types of RIOK2 shRNA are plotted in a bar graph to illustrate the differences between each group. Bars connecting groups represent statistically significant differences relative to the control while the number of asterisks indicates the degree of significance. P-values for conducted t-tests are also included for each bar.

Next, we analyzed the data for *Ink4a/arf*$^{-/-}$; *PTEN*$^{-/-}$; *EGFR*^{vIII} mGSCs infected with the same RIOK2-shRNA or GFP control. Again, Welch's t-tests between the *Ink4a/arf*$^{-/-}$; *PTEN*$^{-/-}$; *EGFR*^{vIII} mGSCs infected with lentivirus containing RIOK2 shRNA groups and those with the GFP control were performed to determine if the shRNA had a significant effect in knocking down *RIOK2* mRNA expression. Although the RIOK2-shRNA2 ($p=0.0015$) showed a statistically significant reduction in relative expression of *RIOK2*, the cells infected with RIOK2-shRNA1 did not exhibit a statistically significant difference in relative *RIOK2* expression compared to the GFP control (data not included).

IHC of Tumor Micoarray (TMA)

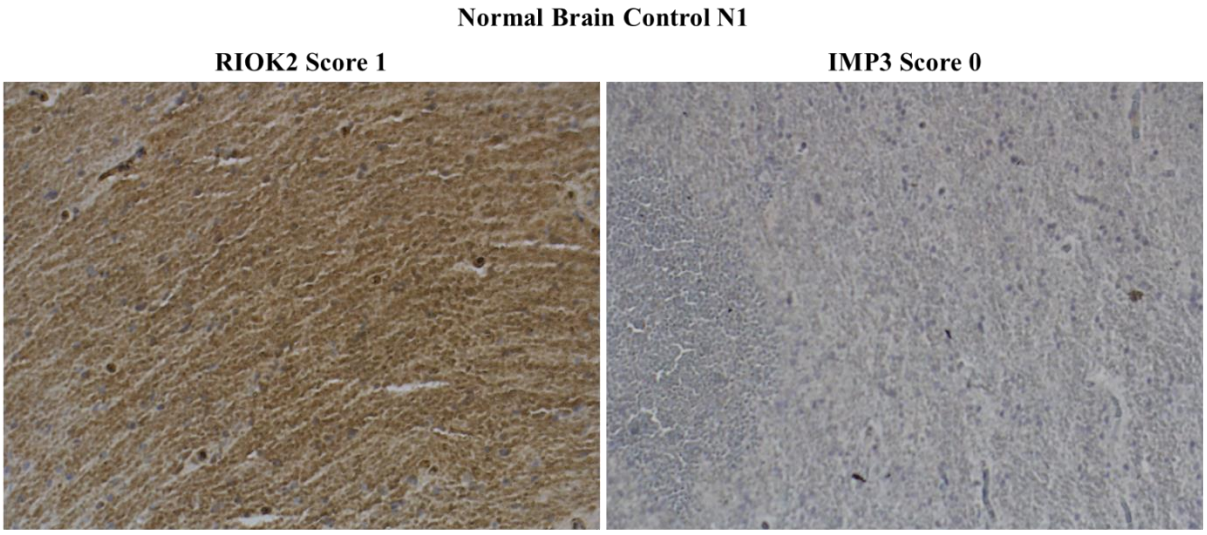

Figure 5. Immunohistochemistry using an HRP-conjugated secondary antibody to either a rabbit anti-RIOK2 (left) or mouse anti-IMP3 (right) primary antibody. Images above were taken at 20X magnification under the same lighting conditions and are of corresponding samples normal brain control (N1) tissue in the TMA.

Available corresponding samples on the TMA slides after completion of the immunohistochemistry process probing for RIOK2 or IMP3 protein expression were scored, imaged, and juxtaposed. Figure 5 illustrates an example sample of the normal brain control (pseudonym N1) with a RIOK2 staining score of 1 and an IMP3 staining score of 0. The relative spatial arrangement of the cells does not seem overly abundant, as would be expected for normal brain tissue relative to tumor. Additionally, the staining of RIOK2 seems to be strongest in the cytoplasm with some nuclear staining, suggesting a largely cytoplasmic localization. There is one cell in the IMP3 image that appears to be expressing IMP3; however, the general score of the sample is a 0 considering that the rest of the tissue did not appear to have any IMP3 expression.

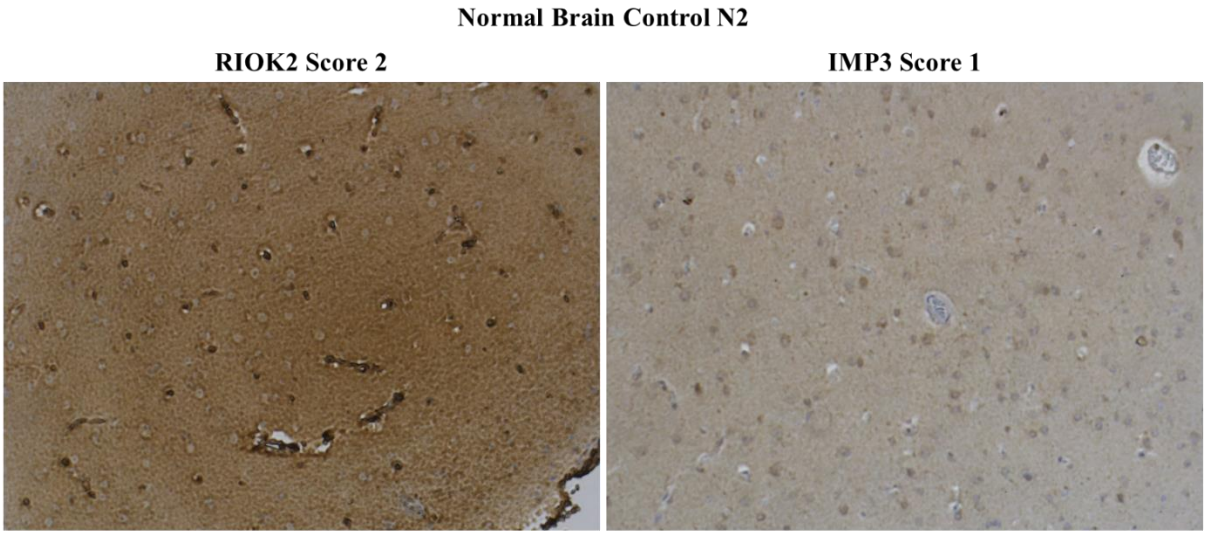

Figure 6. Immunohistochemistry using an HRP-conjugated secondary antibody to either a rabbit anti-RIOK2 (left) or mouse anti-IMP3 (right) primary antibody. Images above were taken at 20X magnification under the same lighting conditions and are of corresponding samples normal brain control (N2) tissue in the TMA.

There were additional corresponding samples of normal brain control tissue between the TMAs (N2) that exhibited low-level expression of IMP3 with higher expression of RIOK2 relative to the N1 control (Figure 6). As in the N1 control, RIOK2 staining appears to be strongest throughout the cytoplasm and nucleus; however, IMP3 expression appears to be largely perinuclear. Staining of the RIOK2 samples also appears to be strongest and fades at the peripheries. Nuclear staining in the RIOK2 TMA is also slightly less clear because of the overlapping expression of RIOK2, though the nuclear staining in the IMP3 TMA shows fewer cell nuclei that are well-spaced.

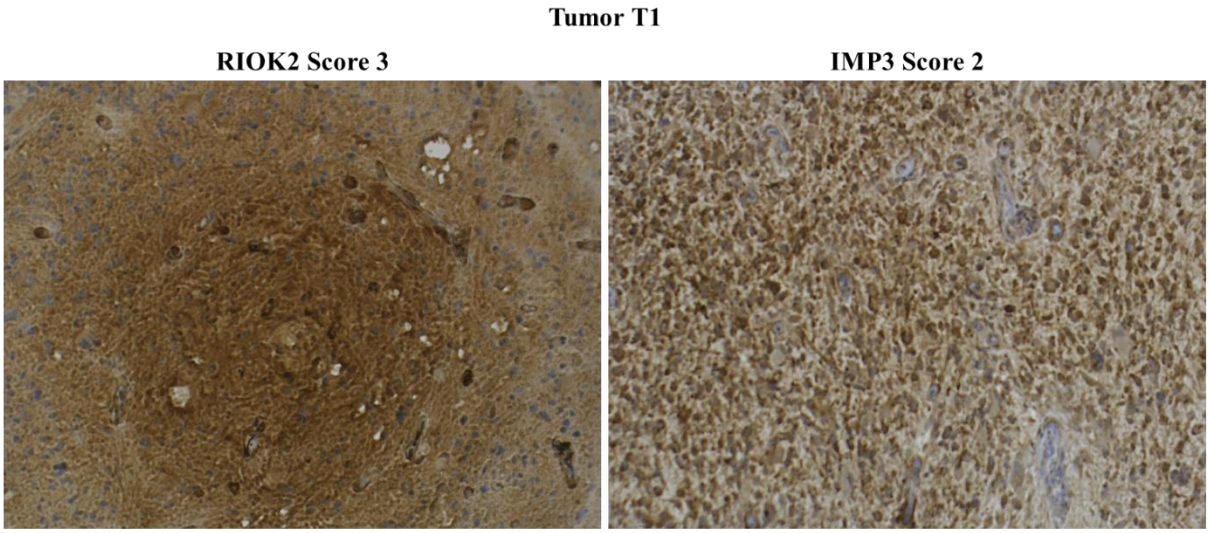

Figure 7. Immunohistochemistry using an HRP-conjugated secondary antibody to either a rabbit anti-RIOK2 (left) or mouse anti-IMP3 (right) primary antibody. Images above were taken at 20X magnification under the same lighting conditions and are of corresponding tumor (T1) samples in the TMA.

Relative to the N1 (Figure 5) and N2 (Figure 6) control samples, corresponding samples of tumor tissue (T1) illustrate increased amounts of nuclear staining in both the RIOK2 TMA and IMP3 TMA (Figure 7). The increased number of cells also appear to have stronger expression of each respective protein, as the T1 samples had a RIOK2 score of 3 and an IMP3 score of 2. RIOK2 expression appears to still be strongest throughout the cytoplasm with lighter staining in the nucleus while IMP3 expression is perinuclear in T1 as before in N2.

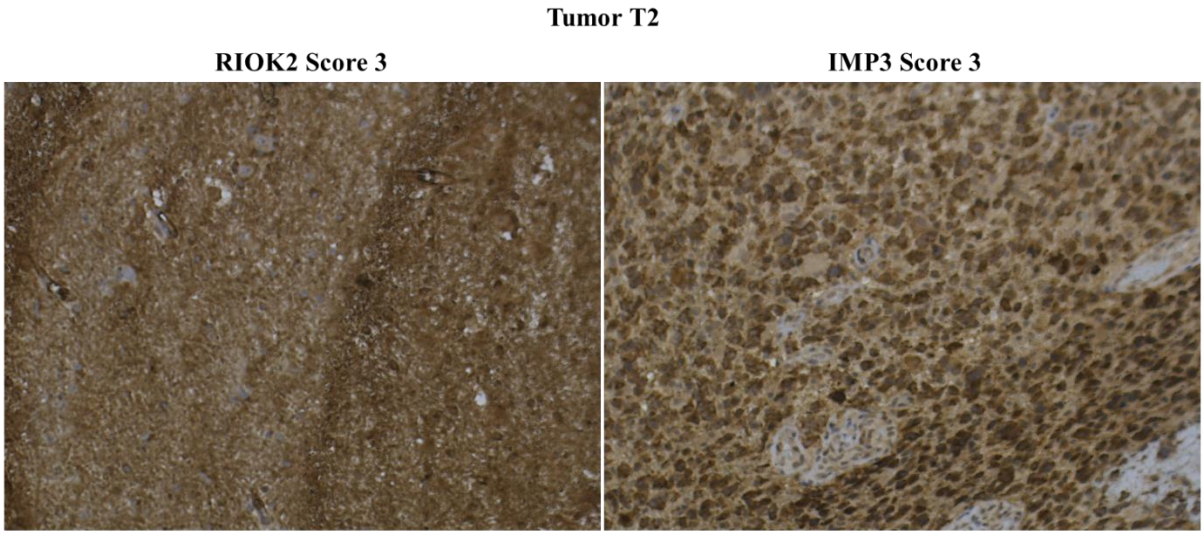

Figure 8. Immunohistochemistry using an HRP-conjugated secondary antibody to either a rabbit anti-RIOK2 (left) or mouse anti-IMP3 (right) primary antibody. Images above were taken at 20X magnification under the same lighting conditions and are of corresponding tumor (T2) samples in the TMA.

RIOK2 and IMP3 staining of the T2 sample recapitulates many of the traits seen in the previous samples, both N2 and T1, strong expression of RIOK2 throughout the cytoplasm and largely perinuclear expression of IMP3 (Figure 8). The staining on the RIOK2 TMA is so strong for the T2 sample that it is more difficult to see the nuclear regions of the cells, and a similar process occurred in the IMP3 TMA. T2 is also the only imaged sample with an available genetic background. Specifically, the sample has an amplification of EGFR and MET, in addition to loss of PTEN.

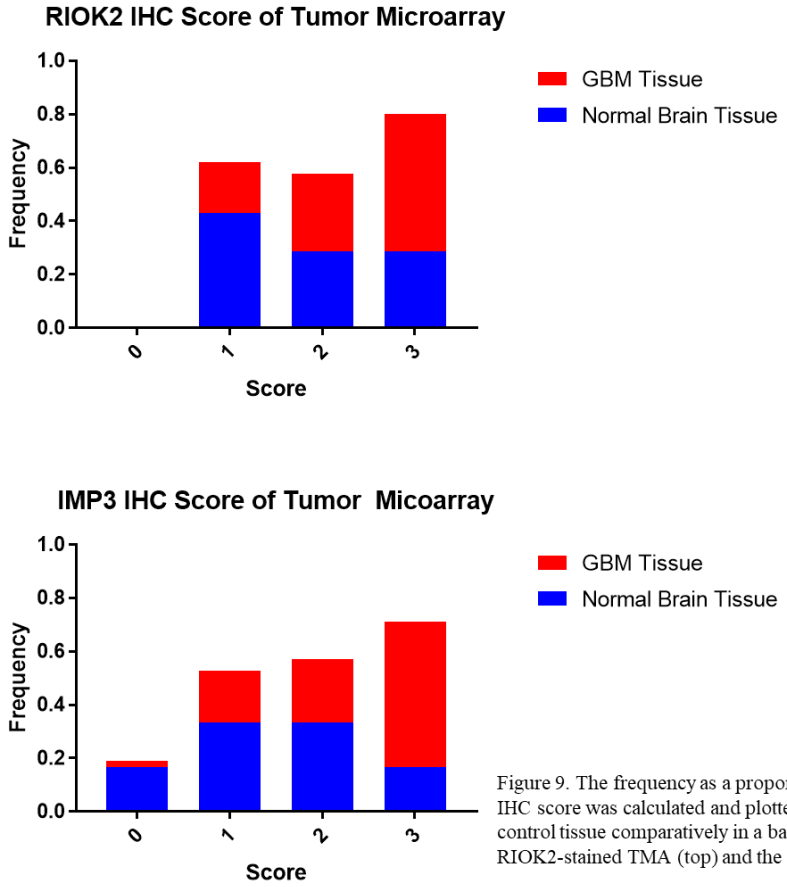

Figure 9. The frequency as a proportion of samples corresponding to each IHC score was calculated and plotted for GBM tissue and normal brain control tissue comparatively in a bar graph. Frequencies were counted for the RIOK2-stained TMA (top) and the IMP3-stained TMA (bottom).

After completing the IHC staining of the RIOK2 TMA and IMP3 TMA, the total number of stained samples remaining on the slides were counted and their scores were analyzed by frequency between tissue types (Figure 9). Of the 108 samples that compose the TMA, 52 samples remained on the IMP3 TMA, 6 of which were normal brain control, and 38 samples remained on the RIOK2 TMA, 7 of which were normal brain control. Of the 46 tumor samples on the IMP3 TMA, the most frequently occurring score was a 3, while there was a tie between the 1 and 2 scores in the normal brain control (Figure 9, bottom). Comparatively, the most frequently occurring score for the RIOK2 TMA samples was a 3 in the tumor tissues and a 1 in the normal brain control.

DISCUSSION

Considering the extremely poor over-all survival rate of patients diagnosed with GBM despite the established standard of care and considerable research progress on the genetic drivers of malignancy, there are significant gaps in our current understanding of this disease (Cloughesy et al., 2008; Hanif et al., 2017; MacDonald et al., 2011). Preliminary data utilizing the *Drosophila* GBM model and human cell-cultured-based models of GBM have identified the catalytic activity of the atypical serine-threonine kinase RIOK2 as being necessary for neoplastic glial cell proliferation and survival (Read et al., 2009; Read et al., 2013). Preliminary experiments in our laboratory have identified the RNA-binding protein IMP3 as a potential effector through which RIOK2 acts in GBM.

To further investigate the relationship between RIOK2 and IMP3 function, mRNA expression data from the TCGA and Gravendeel datasets for *EGFR*, *PDGFR-α*, *RIOK2*, *IMP3*, and *MYC* was gathered and analyzed according to tumor grade and *IDH1*-mutant status (Cancer Genome Atlas Research et al., 2013; Gravendeel et al., 2009). We observed a general trend of increased mRNA expression in ascending grades for the genes screened (Figure 1), and these trends are consistent with published literature on the role of overexpression of RTKs, *RIOK2*, and *IMP3* in higher-grade gliomas (Bell et al., 2013; Lederer et al., 2014; Read et al., 2013). In contrast, *IDH1*-mutant status did not generally correlate with significant differences in expression for *EGFR*, *RIOK2*, or *MYC* (Figure 2). However, there was a statistically significant lower expression of *IMP3* among the *IDH1*-mutant samples ($p=0.0022$). Given that primary GBM is associated with *IDH1*-wild-type status, which has a worse prognosis than secondary *IDH1*-mutant GBM and considering that higher expression of *IMP3* is associated with poor prognosis, this difference seems to be well-supported (Del Gobbo et al., 2015; Ohgaki and Kleihues, 2013).

Although the goals of this project initially included development of the inducible mouse-model of GBM for viral infection with lentivirus or RCAS alongside my postdoc research mentor Dr. Nathaniel Boyd, complications with viral infection rates of the mNSCs and mGSCs using lentivirus delayed our progress. Thus, I focused on validating the knockdown of *RIOK2* in the mNSCs and mGSCs with shRNA administered via lentivirus *in vitro*. *Ink4a/arf*$^{-/-}$ mNSCs and *Ink4a/arf*$^{-/-}$; *PTEN*$^{-/-}$; *EGFR*^{vIII} mGSCs were both infected to examine a potential difference in the expression of RTK-PI3K signaling effectors when *RIOK2* expression is knocked down. RT-qPCR of mRNA isolated from stably infected cells showed a statistically significant decrease in the relative expression of *RIOK2* for both populations in the RIOK2-shRNA2 group ($p=0.0015$ and $p=0.0030$) but did not have a statistically significant decrease in the RIOK2-shRNA1 group of the *ink4a/arf*$^{-/-}$; *PTEN*$^{-/-}$; *EGFR*^{vIII} mGSCs (Figures 3 and 4). The relative amount of actin expression was significantly lower than the GFP control case for the *Ink4a/arf*$^{-/-}$; *PTEN*$^{-/-}$; *EGFR*^{vIII} mGSCs which could explain the dramatically skewed results for the other genes and is likely a byproduct of the shRNA having a synthetic lethal effect on the RTK-PI3K driven cells. These infection experiments will be replicated to further validate the efficiency of lentivirus and to identify the best shRNA sequence for RIOK2 to use going forward in our murine GBM models.

To determine if RIOK2 and IMP3 proteins showed co-overexpression in GBM tumors, I chose to explore the expression of these proteins in a variety of GBM patient tissue samples via immunohistochemistry in a tumor tissue microarray. The samples included in the TMA slides were isolated from several different patients with different tumor genotypes. In the imaged samples (T2 in Figure 8), as shown, we observed strong RIOK2 and IMP3 expression in tissue specimens from tumors which had amplification of EGFR and MET RTKs with a loss of PTEN. Each of these features can upregulate in RTK-PI3K signaling and drive gliomagenesis which might explain why

a tumor sample containing all three of these features would have such high expression of RIOK2 and IMP3.

While the individual TMA slides were useful for preliminary examination at the expression levels of RIOK2 and IMP3 for each of the samples, replicates will be needed to validate our findings and to allow for statistical analysis. The TMA slides stained for this project will also be scored by Dr. Boyd to eliminate bias and neuropathologist Dr. Neill to validate the cell type. Immunohistochemical staining to examine the expression of different signaling effectors like MYC and SOX2 is another future experiment to examine other modules associated with RTK-PI3K signaling and IMP3. Although we were able to optimize the antibody dilutions utilized for RIOK2 (1:125) and IMP3 (1:250), one problem we encountered was the loss of samples on the tumor microarray during washes between antibody incubation steps, a problem which is likely a result of poor adhesion of the tissue samples to our slides. For each slide the TMA should have included 108 samples, yet at most we were able to stain 52 on the IMP3 TMA and 38 on the RIOK2 TMA.

In all, the data generated from this project provides preliminary support for the co-expression of RIOK2 and IMP3 in RTK-PI3K driven GBM. However, time-limitations required that additional experiments will need be performed to complete the initial objectives of this project. Namely, additional immunohistochemistry of the TMAs including replicates of those already processed will provide more data to explore the correlations between RIOK2 and IMP3 expression and expression of their regulators and target genes. The qPCR findings of effective knockdown of RIOK2 in the mNSCs and mGSCs will also need to be replicated prior to moving onto the inducible mouse model of GBM.

TABLE OF FIGURES

REFERENCES

Becher, O.J., Hambardzumyan, D., Fomchenko, E.I., Momota, H., Mainwaring, L., Bleau, A.M., Katz, A.M., Edgar, M., Kenney, A.M., Cordon-Cardo, C., *et al.* (2008). Gli activity correlates with tumor grade in platelet-derived growth factor-induced gliomas. Cancer Res *68*, 2241-2249.

Bell, J.L., Wachter, K., Muhleck, B., Pazaitis, N., Kohn, M., Lederer, M., and Huttelmaier, S. (2013). Insulin-like growth factor 2 mRNA-binding proteins (IGF2BPs): post-transcriptional drivers of cancer progression? Cell Mol Life Sci *70*, 2657-2675.

Bondy, M.L., Scheurer, M.E., Malmer, B., Barnholtz-Sloan, J.S., Davis, F.G., Il'yasova, D., Kruchko, C., McCarthy, B.J., Rajaraman, P., Schwartzbaum, J.A., *et al.* (2008). Brain tumor epidemiology: consensus from the Brain Tumor Epidemiology Consortium. Cancer *113*, 1953-1968.

Bowman, R.L., Wang, Q., Carro, A., Verhaak, R.G., and Squatrito, M. (2017). GlioVis data portal for visualization and analysis of brain tumor expression datasets. Neuro Oncol *19*, 139-141.

Brennan, C.W., Verhaak, R.G., McKenna, A., Campos, B., Noushmehr, H., Salama, S.R., Zheng, S., Chakravarty, D., Sanborn, J.Z., Berman, S.H., *et al.* (2013). The somatic genomic landscape of glioblastoma. Cell *155*, 462-477.

Cancer Genome Atlas Research, N. (2008). Comprehensive genomic characterization defines human glioblastoma genes and core pathways. Nature *455*, 1061-1068.

Cancer Genome Atlas Research, N., Weinstein, J.N., Collisson, E.A., Mills, G.B., Shaw, K.R., Ozenberger, B.A., Ellrott, K., Shmulevich, I., Sander, C., and Stuart, J.M. (2013). The Cancer Genome Atlas Pan-Cancer analysis project. Nat Genet *45*, 1113-1120.

Chen, A.S., Wardwell-Ozgo, J., Shah, N.N., Wright, D., Appin, C.L., Vigneswaran, K., Brat, D.J., Kornblum, H.I., and Read, R.D. (2019). Drak/STK17A Drives Neoplastic Glial Proliferation through Modulation of MRLC Signaling. Cancer Research *79*, 1085-1097.

Cloughesy, T.F., Yoshimoto, K., Nghiemphu, P., Brown, K., Dang, J., Zhu, S., Hsueh, T., Chen, Y., Wang, W., Youngkin, D., *et al.* (2008). Antitumor activity of rapamycin in a Phase I trial for patients with recurrent PTEN-deficient glioblastoma. PLoS Med *5*, e8.

Cohen, A.L., Holmen, S.L., and Colman, H. (2013). IDH1 and IDH2 mutations in gliomas. Curr Neurol Neurosci Rep *13*, 345.

Del Gobbo, A., Vaira, V., Ferrari, L., Patriarca, C., Di Cristofori, A., Ricca, D., Caroli, M., Rampini, P., Bosari, S., and Ferrero, S. (2015). The oncofetal protein IMP3: a novel grading tool and predictor of poor clinical outcome in human gliomas. Biomed Res Int *2015*, 413897.

Gravendeel, L.A.M., Kouwenhoven, M.C.M., Gevaert, O., de Rooi, J.J., Stubbs, A.P., Duijm, J.E., Daemen, A., Bleeker, F.E., Bralten, L.B.C., Kloosterhof, N.K., *et al.* (2009). Intrinsic Gene Expression Profiles of Gliomas Are a Better Predictor of Survival than Histology. Cancer Research *69*, 9065-9072.

Hambardzumyan, D., Amankulor, N.M., Helmy, K.Y., Becher, O.J., and Holland, E.C. (2009). Modeling Adult Gliomas Using RCAS/t-va Technology. Transl Oncol *2*, 89-95.

Hanif, F., Muzaffar, K., Perveen, K., Malhi, S.M., and Simjee Sh, U. (2017). Glioblastoma Multiforme: A Review of its Epidemiology and Pathogenesis through Clinical Presentation and Treatment. Asian Pac J Cancer Prev *18*, 3-9.

Jakel, S., and Dimou, L. (2017). Glial Cells and Their Function in the Adult Brain: A Journey through the History of Their Ablation. Front Cell Neurosci *11*, 24.

Jovcevska, I., Kocevar, N., and Komel, R. (2013). Glioma and glioblastoma - how much do we (not) know? Mol Clin Oncol *1*, 935-941.

Komori, T. (2017). The 2016 WHO Classification of Tumours of the Central Nervous System: The Major Points of Revision. Neurol Med Chir (Tokyo) *57*, 301-311.

Lederer, M., Bley, N., Schleifer, C., and Huttelmaier, S. (2014). The role of the oncofetal IGF2 mRNA-binding protein 3 (IGF2BP3) in cancer. Semin Cancer Biol *29*, 3-12.

Louis, D.N., Holland, E.C., and Cairncross, J.G. (2001). Glioma classification: a molecular reappraisal. Am J Pathol *159*, 779-786.

Louis, D.N., Ohgaki, H., Wiestler, O.D., Cavenee, W.K., Burger, P.C., Jouvet, A., Scheithauer, B.W., and Kleihues, P. (2007). The 2007 WHO classification of tumours of the central nervous system. Acta Neuropathol *114*, 97-109.

MacDonald, T.J., Aguilera, D., and Kramm, C.M. (2011). Treatment of high-grade glioma in children and adolescents. Neuro Oncol *13*, 1049-1058.

Ohgaki, H., and Kleihues, P. (2005). Epidemiology and etiology of gliomas. Acta Neuropathol *109*, 93-108.

Ohgaki, H., and Kleihues, P. (2013). The definition of primary and secondary glioblastoma. Clin Cancer Res *19*, 764-772.

Palanichamy, J.K., Tran, T.M., Howard, J.M., Contreras, J.R., Fernando, T.R., Sterne-Weiler, T., Katzman, S., Toloue, M., Yan, W., Basso, G., *et al.* (2016). RNA-binding protein IGF2BP3 targeting of oncogenic transcripts promotes hematopoietic progenitor proliferation. J Clin Invest *126*, 1495-1511.

Pitter, K.L., Tamagno, I., Alikhanyan, K., Hosni-Ahmed, A., Pattwell, S.S., Donnola, S., Dai, C., Ozawa, T., Chang, M., Chan, T.A., *et al.* (2016). Corticosteroids compromise survival in glioblastoma. Brain *139*, 1458-1471.

Read, R.D., Cavenee, W.K., Furnari, F.B., and Thomas, J.B. (2009). A drosophila model for EGFR-Ras and PI3K-dependent human glioma. PLoS Genet *5*, e1000374.

Read, R.D., Fenton, T.R., Gomez, G.G., Wykosky, J., Vandenberg, S.R., Babic, I., Iwanami, A., Yang, H., Cavenee, W.K., Mischel, P.S., *et al.* (2013). A kinome-wide RNAi screen in Drosophila Glia reveals that the RIO kinases mediate cell proliferation and survival through TORC2-Akt signaling in glioblastoma. PLoS Genet *9*, e1003253.

Regad, T. (2015). Targeting RTK Signaling Pathways in Cancer. Cancers (Basel) *7*, 1758-1784.

Suvasini, R., Shruti, B., Thota, B., Shinde, S.V., Friedmann-Morvinski, D., Nawaz, Z., Prasanna, K.V., Thennarasu, K., Hegde, A.S., Arivazhagan, A., *et al.* (2011). Insulin growth factor-2 binding protein 3 (IGF2BP3) is a glioblastoma-specific marker that activates phosphatidylinositol 3-kinase/mitogen-activated protein kinase (PI3K/MAPK) pathways by modulating IGF-2. J Biol Chem *286*, 25882-25890.

Szulzewsky, F., Pelz, A., Feng, X., Synowitz, M., Markovic, D., Langmann, T., Holtman, I.R., Wang, X., Eggen, B.J., Boddeke, H.W., *et al.* (2015). Glioma-associated microglia/macrophages display an expression profile different from M1 and M2 polarization and highly express Gpnmb and Spp1. PLoS One *10*, e0116644.

Tian, M., Ma, W., Chen, Y., Yu, Y., Zhu, D., Shi, J., and Zhang, Y. (2018). Impact of gender on the survival of patients with glioblastoma. Biosci Rep *38*.

Walker, K., and Hjelmeland, A. (2014). Method for Efficient Transduction of Cancer Stem Cells. J Cancer Stem Cell Res *2*.

Wen, P.Y., and Kesari, S. (2008). Malignant gliomas in adults. N Engl J Med *359*, 492-507.